COPPENS, P., LEISEROWITZ, L. & RABINOVICH, D. (1965). *Acta Cryst.* **18**, 1035-1038.
CRAVEN, B. M. & SABINE, T. M. (1966). *Acta Cryst.* **20**, 214-219.
CROMER, D. T. & LIBERMAN, D. (1970). *J. Chem. Phys.* **53**, 1891-1898.
CROMER, D. T. & MANN, J. B. (1968). *Acta Cryst.* A**24**, 321-324.
DAM, J., HARKEMA, S. & FEIL, D. (1983). *Acta Cryst.* B**39**, 760-768.
DUNNING, T. H. (1970). *J. Chem. Phys.* **53**(7), 2823-2833.
DUNNING, T. H. (1971). *J. Chem. Phys.* **55**(2), 716-723.
GAJHEDE, M. (1985). *Chem. Phys. Lett.* **120**, 266-271.
GUNDERSEN, G. (1981). *Acta Chem. Scand. Ser. A*, **35**, 729-731.
GUPTA, A. & TOSSELL, J. A. (1981). *Phys. Chem. Miner.* **7**, 159-164.
HANSEN, N. K. & COPPENS, P. (1978). *Acta Cryst.* A**34**, 909-921.
HERMANSSON, K. (1984). Thesis, Univ. of Uppsala.
HIRSHFELD, F. L. (1976). *Acta Cryst.* A**32**, 239-244.
International Tables for X-ray Crystallography (1974). Vol. IV, Table 2.2D. (Present distributor D. Reidel, Dordrecht.)
JOHNSON, C. K. (1976). *ORTEP*II. Report ORNL-5138. Oak Ridge National Laboratory, Tennessee.
KIRFEL, A., WILL, G. & STEWART, R. F. (1983). *Acta Cryst.* B**39**, 175-185.
LUNELL, S. (1984). *J. Chem. Phys.* **80**, 6185-6193.
REES, B. (1977). *Isr. J. Chem.* **16**, 180-186.
RETTRUP, S. & SARMA, C. R. (1977). *Theor. Chim. Acta*, **46**, 73-77.
SEILER, P., SCHWEIZER, W. B. & DUNITZ, J. D. (1984). *Acta Cryst.* B**40**, 319-327.
STEWART, J. M. (1976). Editor. The *X-RAY*76 system. Tech. Rep. TR-446. Computer Science Center, Univ. of Maryland, College Park, Maryland.
STEWART, R. F. (1976). *Acta Cryst.* A**32**, 565-574.
STEWART, R. F., DAVIDSON, E. R. & SIMPSON, W. T. (1965). *J. Chem. Phys.* **42**, 3175-3187.
SWAMINATHAN, S., CRAVEN, B. M., SPACKMAN, M. & STEWART, R. F. (1984). *Acta Cryst.* B**40**, 398-404.
YAMABE, S., KITAURA, K. & NISHIMOTO, K. (1978). *Theor. Chim. Acta*, **47**, 111-131.
ZACHARIASEN, W. H. (1954). *Acta Cryst.* **7**, 305-310.

Acta Cryst. (1986). B**42**, 552-557

Deformation Density in Magnesium Sulfite Hexahydrate

BY J. W. BATS, H. FUESS AND Y. ELERMAN*

Institut für Kristallographie und Mineralogie der Universität Frankfurt am Main, Senckenberganlage 30, *D*-6000 *Frankfurt am Main* 1, *Federal Republic of Germany*

(*Received* 8 *January* 1986; *accepted* 4 *July* 1986)

Dedicated to the memory of Professor P. P. Ewald

Abstract

The deformation electron density in $MgSO_3.6H_2O$ has been determined at 120 K from a combination of X-ray and neutron diffraction data. $M_r = 212{\cdot}47$, rhombohedral, $R3$, $a = 5{\cdot}911(1)$ Å, $\alpha = 96{\cdot}25\ (2)^\circ$, $V = 202{\cdot}6\ (1)$ Å^3, $Z = 1$, $D_x = 1{\cdot}742\ (1)$ g cm^{-3}, $F(000) = 112$, $T = 120$ K. Neutron diffraction: $\lambda = 0{\cdot}8977$ Å, $(\sin\theta/\lambda)_{max} = 0{\cdot}945$ Å^{-1}, $\mu = 1{\cdot}590$ cm^{-1}, $R(F) = 0{\cdot}038$ for 2228 reflections. X-ray diffraction: Mo $K\alpha$ radiation, graphite monochromator, $\lambda = 0{\cdot}71069$ Å, $(\sin\theta/\lambda)_{max} = 1{\cdot}15$ Å^{-1}, $\mu = 4{\cdot}70$ cm^{-1}, $R(F) = 0{\cdot}018$ for 3222 observed independent reflections. The non-centrosymmetric space group causes an underestimation of the deformation density when using phase angles from a spherical-atom refinement. A doubly phased difference synthesis assigning phase angles from a multipole refinement to F_{obs} gave a detailed description of the deformation density. The sulfite O atoms carry a negative charge and are considerably expanded compared with free atoms. An extended lone-pair lobe is observed at the apex of the S pyramid. The net charge on the sulfite group is estimated as $-1{\cdot}0\ (2)$ e. Dipole moments of the hydrate groups derived from the multipole coefficients are 2·37 (14) and 2·15 (14) D (1D = $3{\cdot}3 \times 10^{-30}$ C m). The shape of the hydrate O lone-pair lobes is clearly affected by cation and hydrogen-bond interactions.

Introduction

The present work is part of our study of the deformation density in sulfates and related compounds. Experimental results on $Na_2S_2O_3$ and $MgS_2O_3.6H_2O$ have been reported previously (Elerman, Bats & Fuess, 1983; Bats & Fuess, 1986). A qualitative comparison with theoretical density maps was presented elsewhere (Fuess, Bats, Cruickshank & Eisenstein, 1985). In this paper we present our results on a sulfite: $MgSO_3.6H_2O$. Its crystal structure was first described by Flack (1973) and recently refined by a neutron diffraction study at room temperature (Andersen & Lindqvist, 1984). The present work is based on X-ray and neutron diffraction data measured at 120 K.

* Permanent address: Department of Physics, Faculty of Science, University of Ankara, Beseyler-Ankara, Turkey.

0108-7681/86/060552-06$01.50

Experimental

Single crystals grown from aqueous solutions, cell parameters at 120 K refined from setting angles of 25 reflections with $7<\theta<15°$ in the X-ray diffraction experiment.

Neutron diffraction

Crystal dimensions $1·4\times2·5\times2·8$ mm; $\omega/2\theta$ scan; diffractometer D9 at ILL, Grenoble; cryostat described by Allibon, Filhol, Lehmann, Mason & Simms (1981); thermocouple calibrated with a KH_2PO_4 crystal (phase transition at 122·8 K); hemisphere up to $2\theta=100°$; quadrant with $100<2\theta<116°$; *hkl* range: $h\ 0\rightarrow11$, $k\pm11$, $l\pm11$; 2228 reflections; three standard reflections every 50 reflections remained stable; background corrections by profile analysis (Lehmann & Larsen, 1974); numerical absorption correction, transmission range for absorption: 0·644–0·811; equivalent reflections were not averaged to allow for possible differences in extinction corrections; weights according to $w=s^{-2}$ with s the larger value of $\sigma(F)$ or $0·03F$. Structure refinement on F by *ORXFLS* (Busing *et al.*, 1974); reflections with $F^2_{obs}<0$ included with $F_{obs}=0$; scattering lengths from Koester (1977); anisotropic extinction correction according to Coppens & Hamilton (1970), difference from isotropic extinction correction not significant [$g=1·39(6)\times10^{-3}$, $Y_{min}=0·70$]; final $R=0·038$, $wR=0·042$, $S=1·18$.

X-ray diffraction

Crystal $0·26\times0·27\times0·35$ mm; enclosed in capillary; Enraf–Nonius CAD-4 diffractometer and low-temperature device; thermocouple in the cold-gas stream calibrated using phase transition of KH_2PO_4 at 122·8 K; $\omega/2\theta$ scan; full sphere up to $2\theta=80°$; hemisphere for $80<2\theta<110°$; total number of reflections 6747; independent reflections 3245; three standard reflections every 5000 s remained stable; numerical absorption correction; transmission range: 0·872–0·896; range of *hkl*: ±13; averaging of equivalent reflections (*hkl*, *lhk*, *klh*), $R(I)_{int}=0·020$; Friedel reflections were not averaged because of differing contributions of f''; 3222 reflections with $I>0$ used; weighting scheme $w(F)=[\sigma^2(F)+(0·015F)^2]^{-1}$; calculations with *XRAY* system (Stewart, Kruger, Ammon, Dickinson & Hall, 1972); neutral-atom scattering factors and anomalous-dispersion factors from *International Tables for X-ray Crystallography* (1974); scattering factors for H from Stewart, Davidson & Simpson (1965), RHF (relativistic Hartree–Fock) values (*International Tables for X-ray Crystallography*, 1974) used in difference syntheses; isotropic extinction correction (Larson, 1969): $g=4·48(8)\times10^{-3}$, $Y_{min}=0·62$; refinement on F resulted in $R=0·018$, $wR=0·017$, $S=1·36$. Reversal of the polar axis resulted in $R=0·022$, $wR=0·023$ and $S=1·77$ and thus corresponded to the wrong polarity. The refinement was repeated using only high-angle reflections ($\sin\theta/\lambda>0·65$, 0·80, 0·90 and 1·0 Å^{-1}). The parameters of H atoms and the extinction coefficient were fixed in these refinements. The corresponding S values are $S=1·07$, 1·09, 1·11 and 1·09.

Multipole refinement

$MgSO_3.6H_2O$ crystallizes in a non-centrosymmetric space group. Thus the phase angles of the reflections are not restricted to special values. A refinement on the X-ray diffraction data with a spherical-atom model is thus expected to result in phase angles which deviate slightly from their true values. The use of these phase angles in a difference synthesis is expected to underestimate the features of the deformation density. An electron density study of non-centrosymmetric compounds therefore requires refinement of a non-spherical-atom model.

The refinement of the X-ray diffraction data was therefore continued by the multipole refinement program *MOLLY* (Hansen & Coppens, 1978). For S and O, multipoles up to the hexadecapole level ($l=4$) were used although many terms could be fixed by using crystallographic and local-symmetry constraints. Mg was supposed to be spherical and only its valence-shell population was varied. The H atoms were described with a monopole and a bond-directed dipole. The local orthonormal coordinate systems used are shown in Fig. 1. The following symmetry constraints were used for the atomic deformations: S:1m3, O(1): 111, O(2, 3): 1m1. Positional and thermal parameters for H atoms were fixed to values from the neutron diffraction study. The multipole refinement was performed for two models. In model *A* the multipole populations were refined simultaneously with the positional and anisotropic thermal parameters of the non-H atoms, the scale factor and an isotropic extinction factor. In the final stages of the refinement the radial exponents of the Slater-type deformation functions were included. In model *B* the

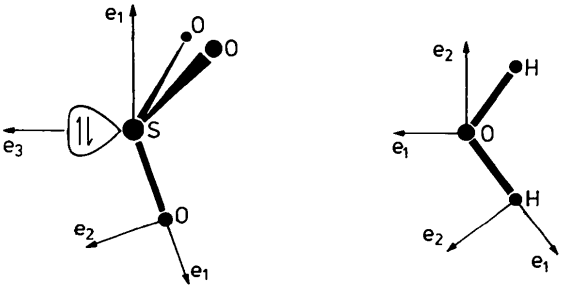

Fig. 1. Local orthonormal coordinate systems used in the multipole refinements. The third axes complete the right-handed coordinate systems.

positional parameters of the O atoms were fixed to the values of the neutron diffraction study while all other parameters were refined as for model *A*. For both models refinement on *F* converged at $R = 0{\cdot}017$, $wR = 0{\cdot}014$ while $S = 1{\cdot}08$ for model *A* and $S = 1{\cdot}10$ for model *B*. A final difference synthesis showed the residual density to be less than 0·08 e Å^{-3}.

Results

The positional parameters of the neutron, conventional and multipole X-ray refinement (model *A*) are compared in Table 1.* The bond distances and angles derived from the neutron diffraction data are given in Table 2, the hydrogen bonds in Table 3. The structure at 120 K is similar to the one at room temperature as refined by Andersen & Lindqvist (1984). The S–O and O–H bonds appear slightly longer at low temperature owing to less vibrational motion while the Mg–O and hydrogen bonds are slightly shorter at low temperature because of shrinkage of the unit cell.

Comparison of the positional parameters of the various conventional, multipole and neutron refinements (Table 1) shows no individual differences exceeding 3σ. As the agreement of the parameter sets is better judged by significance tests, the ten positional parameters of S and O were compared by χ^2 tests. All X-ray refinements (conventional, high order, multipole) show significant differences from the neutron refinement with $\chi^2(XR-N)$ ranging from 25·6 to 35·0. For comparison $\chi^2(\sin\theta/\lambda > 0{\cdot}65-\text{multipole}) = 3{\cdot}8$ indicates fairly good agreement. Moreover, the high-angle and multipole refinements do not approach the neutron positional parameters better than the conventional X-ray refinement. The largest discrepancies occur for atoms O(1) and O(3). Differences in the thermal parameters are more obvious. Those of the neutron determination are systematically smaller than those of the X-ray determination. The overall differences in thermal parameters can be calculated as

$$\Delta U_{ij} = \sum^{\text{atoms}} w[U_{ij}(X) - U_{ij}(N)] / \sum^{\text{atoms}} w$$

and are $\Delta U_{ii} = 0{\cdot}00061(6)$ and $\Delta U_{ij} = 0{\cdot}00032(5)$ for $i \neq j$.

Similar effects are generally found in $X-N$ studies (Elerman, Bats & Fuess, 1983; Coppens *et al.*, 1984), but have never been fully explained. The positional and thermal parameters from the conventional, high-angle ($\sin\theta/\lambda > 0{\cdot}65$ Å^{-1}) and multipole refinements are in perfect agreement.

* Lists of structure factors, anisotropic thermal parameters, multipole parameters and deformation functions have been deposited with the British Library Document Supply Centre as Supplementary Publication No. SUP 43113 (39 pp.). Copies may be obtained through The Executive Secretary, International Union of Crystallography, 5 Abbey Square, Chester CH1 2HU, England.

Table 1. *Positional parameters and equivalent values of the anisotropic thermal parameters*

$$U_{eq} = \tfrac{1}{3}\sum_i\sum_j U_{ij}a_i^*a_j^*\mathbf{a}_i.\mathbf{a}_j.$$

		x	y	z	U_{eq} (Å^2)
Mg	*N*	0·0*	0·0	0·0	0·00694 (12)
	X	0·0	0·0	0·0	0·00718 (3)
	M	0·0	0·0	0·0	0·00720 (2)
S	*N*	−0·50281 (19)	−0·50281	−0·50281	0·00755 (21)
	X	−0·50313 (3)	−0·50313	−0·50313	0·00832 (2)
	M	−0·50312 (2)	−0·50312	−0·50312	0·00836 (2)
O(1)	*N*	−0·25489 (10)	−0·48273 (11)	−0·55929 (11)	0·01023 (18)
	X	−0·25462 (5)	−0·48274 (5)	−0·55935 (5)	0·01095 (6)
	M	−0·25463 (5)	−0·48277 (4)	−0·55934 (4)	0·01095 (7)
O(2)	*N*	−0·14488 (10)	−0·32975 (10)	0·04913 (10)	0·00962 (20)
	X	−0·14493 (4)	−0·32984 (4)	0·04902 (5)	0·01025 (7)
	M	−0·14486 (5)	−0·32982 (4)	0·04906 (4)	0·01024 (7)
O(3)	*N*	0·12320 (10)	0·31789 (10)	−0·07641 (11)	0·01227 (22)
	X	0·12289 (5)	0·31765 (4)	−0·07661 (5)	0·01296 (10)
	M	0·12283 (4)	0·31762 (5)	−0·07655 (5)	0·01300 (9)
H(1)	*N*	−0·1911 (2)	−0·3680 (2)	0·1976 (2)	0·0220 (5)
H(2)	*N*	−0·2743 (2)	−0·4036 (2)	−0·0663 (2)	0·0216 (4)
H(3)	*N*	0·0588 (2)	0·4550 (2)	−0·0246 (3)	0·0270 (7)
H(4)	*N*	0·2638 (2)	0·3659 (2)	−0·1398 (3)	0·0239 (6)

* Fixed to define origin. *N*: neutron refinement; *X*: X-ray refinement ($\sin\theta/\lambda > 0{\cdot}65$ Å^{-1}); *M*: multipole refinement (*A*).

Table 2. *Bond distances* (Å) *and angles* (°) *from the neutron refinement*

3×	Mg–O(2)	2·1063 (7)	3×	O(2)–Mg–O(3)	174·72 (3)
3×	Mg–O(3)	2·0552 (7)	3×	O(2)–Mg–O(2)	86·61 (2)
3×	S–O(1)	1·533 (1)	3×	O(2)–Mg–O(3)	89·35 (3)
	O(2)–H(1)	0·988 (1)	3×	O(2)–Mg–O(3)	89·76 (3)
	O(2)–H(2)	0·992 (1)	3×	O(3)–Mg–O(3)	94·04 (3)
	O(3)–H(3)	0·968 (1)	3×	O(1)–S–O(1)	103·85 (5)
	O(3)–H(4)	0·974 (2)		H(1)–O(2)–H(2)	104·56 (11)
				H(3)–O(3)–H(4)	107·54 (12)

Table 3. *Hydrogen bonds*

	O–H (Å)	H···O (Å)	O···O (Å)	O–H···O (°)
O(2)–H(1)···O(1)	0·988 (1)	1·716 (1)	2·693 (1)	169·2 (1)
O(2)–H(2)···O(1)	0·992 (1)	1·687 (1)	2·675 (1)	173·1 (1)
O(3)–H(3)···O(2)	0·968 (1)	1·892 (2)	2·835 (1)	164·1 (1)
O(3)–H(4)···O(1)	0·974 (2)	1·746 (2)	2·720 (1)	177·9 (1)

Deformation density

The deformation density has been calculated by Fourier synthesis using data up to $\sin\theta/\lambda = 0{\cdot}9$ Å^{-1}. Each F_{obs} value was corrected for anomalous dispersion in a way similar to that described by Yang & Coppens (1974). Subsequently, Friedel reflections were averaged before being used in the Fourier synthesis. The atomic parameters of the O and H atoms were from the neutron determination. Modified thermal parameters defined as $U_{ij}(\text{mod}) = U_{ij}(N) + \Delta U_{ij}$ were used. The parameters of Mg and S have larger errors in the neutron than in the X-ray refinement. Therefore, atomic parameters from a high-order X-ray refinement ($\sin\theta/\lambda > 0{\cdot}9$ Å^{-1}) were used. As the valence density of Mg and S is known to be rather diffuse, this procedure seems justified. The scale factor was taken from the multipole refinement and differs no more than 0·2% from the value of the conventional X-ray refinement. The resulting deformation density in the O–S–O section is shown in Fig. 2(*a*).

As the space group is non-centrosymmetric the phase angles of the observed structure factors may differ from those of the spherical-atom model, normally used for phasing. This phase problem can be avoided by using a doubly phased map in which $|F_{obs}|$ has the phase angle of the multipole refinement and $|F_{calc}|$ the phase angle of the spherical-atom refinement. As seen in Fig. 2(*a*), the single-phase difference density is surprisingly featureless, while use of the doubly phased Fourier synthesis (Fig. 2*b*) shows the deformation density features such as bond and lone-pair peaks very similar to those found in centrosymmetric thiosulfates (Bats & Fuess, 1986). Thus for charge-density studies of non-centrosymmetric structures it is essential to derive the phase angle of $|F_{obs}|$ from a non-spherical-atom model, such as a multipole refinement. An underestimation of the deformation density in non-centrosymmetric structures by using singly phased difference Fourier maps has also been observed in $LiHCOO.H_2O$ (Thomas, 1978) and urea (Swaminathan, Craven, Spackman & Stewart, 1984).

The phase difference $|\overline{\Delta\varphi}| = |\varphi_{multipole} - \varphi_{sph.\ atom}|$ averaged over reflections in $\sin\theta/\lambda$ segments of 0·1 Å^{-1} is shown in Fig. 3. The largest differences ($|\overline{\Delta\varphi}| = 3{\cdot}7°$) are observed for $0{\cdot}2 < \sin\theta/\lambda < 0{\cdot}3$ Å^{-1}. They gradually decrease at larger diffraction angles.

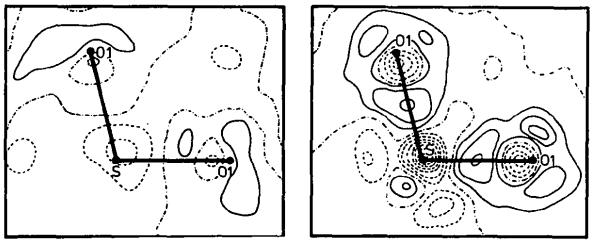

Fig. 2. $X-N$ (in part $X-X$) deformation density in $MgSO_3.6H_2O$. Resolution: $\sin\theta/\lambda = 0{\cdot}90$ Å^{-1}. Contour interval 0·1 e Å^{-3}, negative contours dashed, zero contour dot-dashed. (*a*) Phase angles from spherical-atom refinement; (*b*) doubly phased difference synthesis with phase angles from multipole refinement (*B*) assigned to F_{obs}.

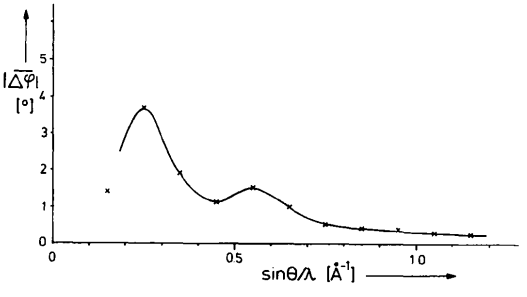

Fig. 3. The phase difference $|\overline{\Delta\varphi}| = |\varphi_{multipole} - \varphi_{sph.\ atom}|$ as a function of $\sin\theta/\lambda$.

As uncertainties in the rescaling of the thermal parameters may introduce systematic errors in the $X-N$ deformation density, it is worthwhile to consider the dynamic model density as well. This density is defined as $\Delta\rho_{model} = \rho_{multipole} - \rho_{sph.\ atom}$, where positional and anisotropic thermal parameters assigned to the spherical atoms are as in the multipole refinement. Fig. 4 shows the dynamic density in the O–S–O section for both multipole models *A* and *B*. It is obvious from this figure that in model *A* where the O positional parameters have been refined simultaneously with the multipole coefficients a rather flat density is observed at O(1). Model *B*, where the O positions were fixed to values from the neutron determination, shows considerably more features near O(1). Moreover, model *B* produces a deformation density in very good agreement with the $X-N$ deformation density. Obviously, the deformation density shows a rather steep curvature near atom O(1), which causes a bias in the atomic parameters in the refinement on the X-ray data. Thus one has to rely on atomic parameters from neutron diffraction or use X-ray data collected at much higher resolution than used in the present study. The same effect was observed for the O atoms in thiosulfates (Bats & Fuess, 1986). Thus model *A* can be rejected. For the water molecules the differences between models *A* and *B* were much smaller. This indicates that the deformation density near the water O atoms is less steep than near the sulfate O atom.

Discussion

The dynamic density (model *B*) shows a pronounced S lone-pair lobe at the apex of the SO_3^{2-} pyramid (Fig. 5). Sections through S–O bonds exhibit a deformation density similar to sulfates (Kirfel & Will, 1980, 1981) and thiosulfates (Bats & Fuess, 1986), although the S–O bond is about 0·05 Å longer in the sulfite anion.

The S atom shows a marked migration of density from the back of the atom into the S–O bonds and the lone-pair lobe. A single peak of about 0·30 e Å^{-3} is found at the midpoint of the S–O bond. The O

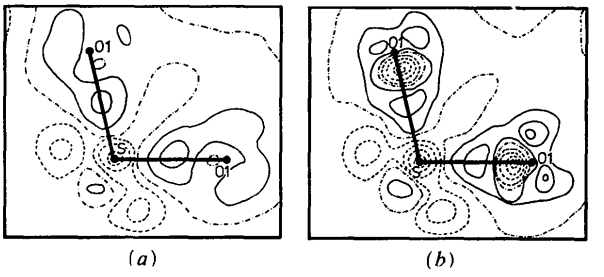

Fig. 4. Dynamic model density in $MgSO_3.6H_2O$. Resolution: $\sin\theta/\lambda = 1{\cdot}0$ Å^{-1}. Contours as in Fig. 2. (*a*) Model *A*; (*b*) model *B*.

atom shows a deep trough at a distance of 0·20 Å from the nuclear position into the O–S bond. This feature is also found in sulfates. This polarization of the O atom will be responsible for the asphericity shift of the atom in the X-ray refinement. The O atom is embedded in a cloud of excess electron density and shows the electronegative O atom to be considerably expanded in comparison with a free atom. This agrees with the refined value of the valence-shell expansion: $\kappa = 0{\cdot}978(3)$. The O lone-pair electron density has its maximum in a doughnut-shaped ring about the S–O bond and forms an angle of about 100° with the S–O bond. Therefore, the O atom appears mainly unhybridized. The O lone-pair lobe appears more concentrated in the section containing the S lone-pair lobe. This would be reasonable if the two Op_π orbitals do not contribute equally to the π bonding in the S–O bonds.

The deformation density in the two independent hydrate groups has peaks of 0·4 e Å^{-3} in the O–H bond (Fig. 6). Electron-deficient regions at the back of the H atoms are directed towards the electron-rich regions of the hydrogen-bond acceptors. The O lone-pair density is considerably extended normal to the HOH plane. There is an obvious correlation between the shape of the lone-pair lobe and the coordination type of the water molecules. O(2) accepts an Mg–O bond and a hydrogen bond. The approximate tetrahedral environment of O(2) is reflected in two separate lone-pair maxima as expected for an sp^3-hybridized atom. O(3) on the other hand accepts only an Mg–O bond which lies almost in the HOH plane. Thus the environment of O(3) is better described as trigonal. The lone-pair lobe of O(3) has only a single maximum directed toward the Mg atom. A similar effect of the crystalline environment on the hydrate lone-pair density was found in $MgS_2O_3.6H_2O$ (Elerman, Bats & Fuess, 1983; Bats & Fuess, 1986) and supports the present result.

Net atomic charges taken from the multipole refinement are given in Table 4. Care has to be taken in the interpretation of these numbers. As shown by Bats & Fuess (1986) net atomic charges may depend considerably on the spatial partitioning method employed. Qualitative trends are nevertheless observed. The net charge on the SO_3 group of −1·0(2) e is less than expected for a pure ionic model, but still accounts for a considerable charge transfer between cation and anion in the expected direction. The negative charge of the anion is concentrated on the O atoms in agreement with the deformation density maps. The overall charge of the S atom is positive notwithstanding the electron-rich lone-pair lobe. The hydrate groups appear almost neutral but are strongly polarized. Dipole moments on the water molecules derived from the multipole coefficients are 2·37(14) and 2·15(14) D, respectively. These values are slightly larger than the expectation value for a free H_2O molecule: $\mu = 1{\cdot}85$ D. Larger than expected dipole moments (2·2–2·4 D) have also been observed by multipole refinements on $MgS_2O_3.6H_2O$ (Bats & Fuess, 1986) and α-oxalic acid dihydrate (Stevens &

Table 4. *Net atomic charges and dipole moments from multipole refinement*

Net charges (e)			
Mg	+0·94 (23)	O(3)	−0·58 (4)
S	+0·43 (11)	H(1)	+0·32 (3)
O(1)	−0·47 (5)	H(2)	+0·37 (3)
O(2)	−0·72 (5)	H(3)	+0·27 (3)
H_2O(I)	−0·03 (6)	H(4)	+0·35 (3)
H_2O(II)	+0·04 (6)		
SO_3	−1·0 (2)		
Dipole moments (D)			
H_2O(I)	2·37 (14)		
H_2O(II)	2·15 (14)		

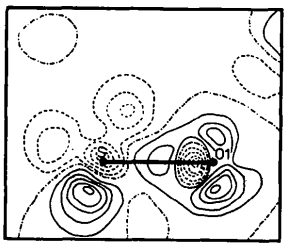

Fig. 5. Dynamic model (*B*) density of the sulfite group in a section containing the S–O bond and the threefold axis. Contours as in Fig. 2.

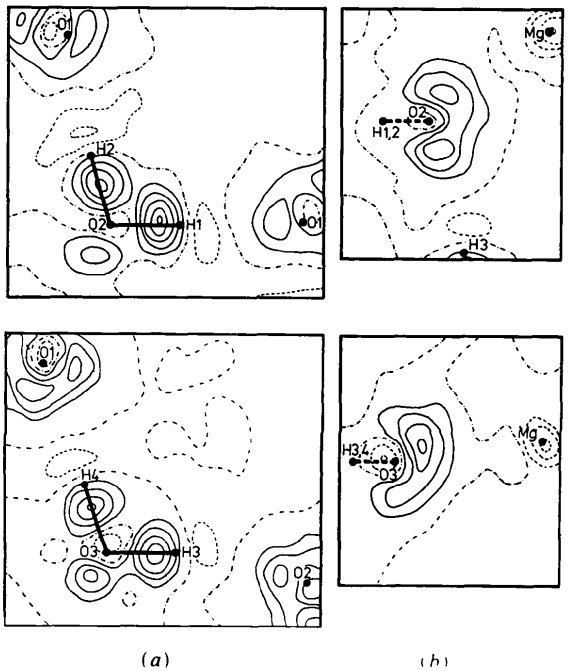

Fig. 6. Doubly phased $X-N$ deformation density in sections containing the hydrate groups. Resolution: $\sin\theta/\lambda = 0{\cdot}90$ Å^{-1}, contours as in Fig. 2. (*a*) The plane defined by the HOH group; (*b*) the plane bisecting the OH bonds.

Coppens, 1980). In those studies somewhat smaller values were observed by discrete boundary-integration methods, where tail-cutting effects occur. Thus the rather large dipole moments in the present study may be an artefact of the real-space partitioning method. The conclusion that the dipole moment of a water molecule increases on hydrate formation may therefore be misleading.

This work was supported by the Bundesminister für Forschung und Technologie of the Federal Republic of Germany.

References

ALLIBON, J. R., FILHOL, F. K., LEHMANN, M. S., MASON, S. A. & SIMMS, P. (1981). *J. Appl. Cryst.* **14**, 326-329.

ANDERSEN, L. & LINDQVIST, O. (1984). *Acta Cryst.* C**40**, 584-586.

BATS, J. W. & FUESS, H. (1986). *Acta Cryst.* B**42**, 26-32.

BUSING, W. R., MARTIN, K. O., LEVY, H. A., BROWN, G. M., ELLISON, R. D., HAMILTON, W. C., IBERS, J. A., JOHNSON, C. K. & THIESSEN, W. E. (1974). *ORXFLS3*. Oak Ridge National Laboratory, Tennessee.

COPPENS, P., DAM, J., HARKEMA, S., FEIL, D., FELD, R., LEHMANN, M. S., GODDARD, R., KRÜGER, C., HELLNER, E., JOHANSEN, H., LARSEN, F. K., KOETZLE, T. F., MCMULLEN, R. K., MASLEN, E. N. & STEVENS, E. D. (1984). *Acta Cryst.* A**40**, 184-195.

COPPENS, P. & HAMILTON, W. C. (1970). *Acta Cryst.* A**26**, 71-83.

ELERMAN, Y., BATS, J. W. & FUESS, H. (1983). *Acta Cryst.* C**39**, 515-518.

FLACK, H. (1973). *Acta Cryst.* B**29**, 656-658.

FUESS, H., BATS, J. W., CRUICKSHANK, D. W. J. & EISENSTEIN, M. (1985). *Angew. Chem. Int. Ed. Engl.* **24**, 509-510.

HANSEN, N. K. & COPPENS, P. (1978). *Acta Cryst.* A**34**, 909-921.

International Tables for X-ray Crystallography (1974). Vol. IV. Birmingham: Kynoch Press. (Present distributor D. Reidel, Dordrecht.)

KIRFEL, A. & WILL, G. (1980). *Acta Cryst.* B**36**, 512-523.

KIRFEL, A. & WILL, G. (1981). *Acta Cryst.* B**37**, 525-532.

KOESTER, L. (1977). *Neutron Physics. Springer Tracts in Modern Physics*, Vol. 80, edited by G. HÖHLER. Berlin: Springer-Verlag.

LARSON, A. C. (1969). In *Crystallographic Computing*, edited by F. R. AHMED, pp. 291-294. Copenhagen: Munksgaard.

LEHMANN, M. S. & LARSEN, F. K. (1974). *Acta Cryst.* A**30**, 580-584.

STEVENS, E. D. & COPPENS, P. (1980). *Acta Cryst.* B**36**, 1864-1876.

STEWART, J. M., KRUGER, G. J., AMMON, H. L., DICKINSON, C. & HALL, S. R. (1972). The *XRAY* system-version of June 1972. Tech. Rep. TR-192. Computer Science Center, Univ. of Maryland, College Park, Maryland.

STEWART, R. F., DAVIDSON, E. R. & SIMPSON, W. T. (1965). *J. Chem. Phys.* **42**, 3175-3187.

SWAMINATHAN, S., CRAVEN, B. M., SPACKMAN, M. A. & STEWART, R. F. (1984). *Acta Cryst.* B**40**, 398-404.

THOMAS, J. O. (1978). *Acta Cryst.* A**34**, 819-823.

YANG, Y. W. & COPPENS, P. (1974). *Solid State Commun.* **15**, 1555-1559.

Acta Cryst. (1986). B**42**, 557-564

MX_5-Ketten aus eckenverknüpften Oktaedern. Mögliche Kettenkonfigurationen und mögliche Kristallstrukturen bei dichtester Packung der X-Atome

VON ULRICH MÜLLER

Fachbereich Chemie der Universität Marburg, Hans-Meerwein-Straße, D-3550 Marburg, Bundesrepublik Deutschland

(*Eingegangen am* 25. *Oktober* 1985; *angenommen am* 21. *Juli* 1986)

Abstract

The possible chain configurations for compounds of the composition MX_5 consisting of chains or rings of vertex-sharing octahedra are derived under the condition that the X atoms form a close-packing arrangement. A group of three connected octahedra can adopt several configuration types having characteristic $M\cdots M\cdots M$ angles; they are designated, in order of decreasing angles, by the following symbols: *cis*-octahedra, hexagonal close packing, *d*, *w*, *v*, *n* and *a*; *cis*-octahedra, *hc* sequence of X atoms, *p* and *q*; *cis*-octahedra, cubic close packing, *r*; *trans*-octahedra, h.c.p., *l* and *k*; *trans*-octahedra, *hc* sequence, *f*; *trans*-octahedra, c.c.p., *t*. For cubic close packing and *cis*-octahedra, sequences of four octahedra must be considered and are given the symbols *e*, *z* and *s*. The configuration types *k*, *w*, *d*, *n*, *a*, *f*, *p* and *q* are chiral, their enantiomeric counterparts being marked by an asterisk. The configuration of any MX_5 chain or ring can be characterized by a sequence of the symbols. The simpler chain types are illustrated. Most of them cannot be packed closely, but one close-packing manner is possible for each of the chains l_2, a_2, t_1 and $f_2f_2^*$, and the rings $(vw)_2$, *anan** and z_4. The ring *vqrq** allows close packing in two ways and the chains w_2 and e_2 in an infinite number of ways. The known structure types of $(RuF_5)_4$ (ring *anan**), $(NbF_5)_4$ (ring z_4), $(SbF_5)_4$ (ring *vqrq**) and α-UF_5 (chain t_1) correspond to the predicted possibilities; $BrF_4Sb_2F_{11}$ fits one of the e_2 chain-packing possibilities. The VF_5 structure type has distorted v_2 chains that do not allow close packing.

0108-7681/86/060557-08$01.50